Application of DOE and ANOVA in optimization of HVOF spraying parameters in the development of new Ti coatings

N. Pulido-González, S. García-Rodríguez, M. Campo, J. Rams and B. Torres*

Dept. de Matemática Aplicada, Ciencia e Ingeniería de Materiales y Tecnología Electrónica, ESCET, Universidad Rey Juan Carlos. C/ Tulipán s/n, Móstoles 28933 Madrid (Spain).

**Corresponding author: Dr. Belen Torres; belen.torres@urjc.es*

Abstract

High Velocity Oxygen-Fuel (HVOF) thermal spray technique has been used to develop new Ti coatings on 1045 steel and 316L stainless steel for different applications. **O**ptimization of the HVOF parameters require**s** numerous experiments to perform, that can be reduced using the Taguchi Design Of Experiment (DOE) methodology. By using DOE, it has been possible to identify the effects of the HVOF spraying parameters (spraying distance, number of layers, gun speed, powder feed rate, type of substrate and type of combustion) **on** the main characteristics of the coatings (porosity, thickness, hardness and adhesion). According to Taguchi method, the resulting orthogonal matrix corresponded to a L16 (4^4 x 2^2) matrix. Using this matrix, the number of experiments was reduced from 1024 to 16 and a first approximation of the best conditions for a real application was obtained. To evaluate the significant spraying variables, a statistical analysis of variance (ANOVA) was used. It has been determined that there is a relationship between coating characteristics and HVOF parameters. Also, the influence of the parameters on the characteristics and properties of the coatings (from high to low) was as follows: spraying distance, number of layers, gun speed, powder feed rate, type of substrate and mixture of gases used in the process.

Keywords

Thermal spray; HVOF; DOE; ANOVA; Titanium; Steel; Stainless steel; Coating;

1. Introduction

Surface engineering provides an alternative that enables the combined use of a substrate with a reasonable cost and a coating with completely different mechanical and chemical properties with the substrate. The use of coatings is one of the most effective strategies to modify the surface properties. The deposition of a new material on the surface using techniques such as PVD (Physical Vapour Deposition), TRD (Thermo Reactive Diffusion) and CVD (Chemical Vapour Deposition) is expensive and presents limited flexibility. The advantage of CVD compared to the other mentioned techniques is the possibility of covering large areas with complex shapes. However, it requires high processing temperatures (800-1000 ^{o}C) whereas the PACVD technique (Plasma Assisted Chemical Vapour Deposition) achieves deposition at lower temperatures, but with more defects [1]–[4].

Thermal spray processes include a number of techniques such as plasma, cold spray and HVOF that are widely and industrially used to obtain coatings on many different types of substrates for a great variety of applications. These techniques are flexible and provide high quality coatings with lower cost than other techniques [1], [2]. The flexibility and superior quality of the coatings obtained by HVOF have made it the excellent choice for many industries, compared with other thermal spraying techniques. The main difficulty of the thermal spray technique is to optimise the multiple variables of the process for each substrate-coating system. Furthermore, the optimum coating characteristics (thickness, porosity, etc.) are different according to the final application. Thermal spray coatings are often applied for better corrosion and wear resistance. Therefore, low porosity and good adhesion are desired properties for the coating. For this reason, HVOF is one of the preferred methods for producing coatings with such characteristics.

The Design Of Experiments (DOE) using Taguchi approach is a powerful tool that allows to simplify and minimize the number of required tests to optimise a system and therefore, it implies a significant reduction of time. It consists of an experimental strategy that studies simultaneously the effects of multiple factors at different levels [5]. Factors are defined as the variables with a direct influence on the process being investigated, while the levels are constituted by the values that the factor takes during experiments. This method designs an orthogonal array showing the necessary experiments to perform. The analysis of variance (ANOVA) is used to determine the response magnitude of each variable (in %) in the orthogonal array previously defined [6]. According to this concrete research, the spraying parameters should be optimised in order to obtain coatings with the desired properties. Several authors have used this methodology in similar processes [7]–[10].

Ti coatings are widely used as they are highly resistant to corrosion and they are biocompatible. An industrial application of these Ti coatings consists of preventing the corrosion caused in the steel pipes by molten aluminium, where several ceramic and intermetallic coatings (Al_2O_3, Al_2TiO_5, CrC, TiO_2, $MoSi_2$, Mg_2SiO_4, Cr_3Si, MgO+ZrO_2, Al_2O_3, MgO, Y_2O_3, ZrO_2, W, CW, SiC, $ZrSiO_4$, Cr_2O_3+Al_2O_3, Y_2O_3+ZrO) have been used [11], [12]. However, they present the disadvantage of having a greater thermal expansion coefficient (CTE) compared to steel [2], [13]–[18]. Ti coatings would be an interesting alternative since they possess a CTE closer to that of a steel substrate. On the other hand, the use of Ti coatings in the biomedical industry for implants, dental and orthopaedic applications is found as an ideal solution due to its excellent biocompatibility, appropriate mechanical properties and corrosion resistance [19]–[21].

The manufacture of Ti coatings on steel substrates using spraying techniques has been dealt with by different authors [22]–[24], which used modified spraying systems, such as warm spraying and cold spraying, to obtain coatings that enable low levels of oxidation. A rise in the particle

temperature leads to an exponential increment in the oxidation level. For this reason, the control of the temperature is important, and it can be reduced by means of CGDS (Cold Gas Dynamic Spray) systems, although not very efficiently, as coatings are obtained with higher degree of porosity.

There are no previous reports in the literature on the analysis of the HVOF coating process of Ti using different statistical tools such as DOE using Taguchi approach and ANOVA. In this study, we propose the deposition of Ti coatings using HVOF, which enables spraying different types of materials at supersonic speeds to obtain compact coatings on all types of substrates. Porosity and oxidation are controllable by modifying the spraying variables and the proportion of combustion gases (O_2/H_2).

To achieve versatile coatings (greater or lower porosity, oxidation, etc.) according to the application, it is necessary to control the technique by optimising the studied variables, in our case for the Steel/Ti system. In this research, the DOE using the Taguchi approach has been employed to evaluate the influence of the spraying parameters (spraying distance, number of deposited layers, gun speed, percentage of feeding powder, type of substrate, type of combustion) on the characteristics and properties of the coatings formed (thickness, porosity, substrate-coating adhesion and micro-hardness). The result is an L16 orthogonal array (4^4 x 2^2), which reduces the number of necessary experiments to 16. Achieving the 16 different conditions leads to the optimization of the spraying parameters, obtaining coatings with the required characteristics.

2. Experimental procedure

2.1. Materials

Commercial carbon steel 1045 and stainless steel 316L (Fundiciones Gómez S.A, Spain, Europe) supplied in bars with a section of 25 mm x 5 mm were used as substrates.

99.5% pure titanium powder from Sulzer Metco 4017 (Oerlikon Metco Europe GmbH, Germany, Europe) was used as the coating material. The morphology of the particles is angular (Figure 1) and the measured average size distribution was 60 ± 6 □m that is in the range (from 53 to 180 □m) given by the supplier. This powder is suitable for both metallic and biocompatible coatings.

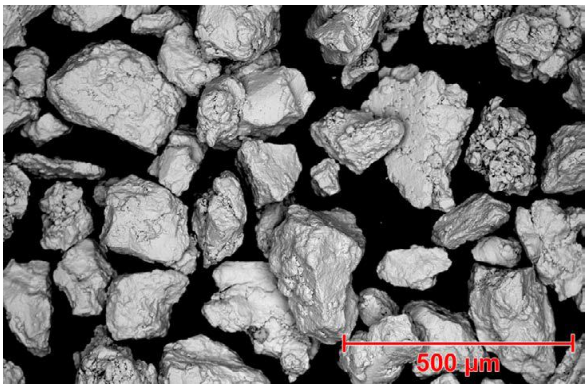

Figure 1. SEM-BSE micrograph of the Ti powder used as coating material.

2.2. Spraying conditions and Taguchi Method.

Titanium coatings were deposited onto carbon steel and stainless steel substrates surfaces using HVOF thermal spray equipment Unicoat DJ2600 from Sulzer Metco (Oerlikon Metco Europe GmbH, Germany, Europe). The spraying gun, a Diamond Jet Sulzer Metco 52C-NS (Oerlikon Metco Europe GmbH, Germany, Europe), was placed on an anthropomorphic robot ABB IRB-2004/16 to control the different spraying variables. Before coating deposition, the substrate surface was sandblasted with alumina particles of an average size of 1 mm and preheated. The preheating consists of one spraying gun pass over all the specimen surface without spraying powder.

To establish the number of experiments to carry out, the MINITAB 17 program designed to perform basic and advanced statistical functions was used. This software allows the use of the Taguchi DOE analysis, which was used to evaluate the influence of the HVOF parameters on the characteristics and properties of the coatings.

A mixed-level design was selected in Taguchi method (see Table 1):

- Four factors (spraying distance, number of layers, gun speed and powder feed rate) with four levels for each factor (200, 250, 300, 350 mm; 6, 9, 12, 15 layers; 100, 150, 200, 250 mm/s; 20, 30, 40, 50 %) respectively.
- Two factors (type of substrate and O_2/H_2 ratio) with two levels for each factor.

These factors and levels were used to design an orthogonal matrix L16 (4^4 x 2^2). The total number of possible experiments is 1024. Using the Taguchi DOE analysis, the number of required experiments decreases to 16, which are presented in Table 2.

Two types of mixture gases were used: the first one presents greater amount of oxygen than hydrogen O_2/H_2 = 130 NLPM / 570 NLPM (hereinafter called “Oxi.”) and the second one, presents less amount of oxygen than hydrogen O_2/H_2 = 147 NLPM / 717 NLPM (hereinafter called “Red.”). The spacing between passes was 10 mm for all deposited coatings.

Table 1. Factors and levels used for experimentation.

Variable	Value
Spraying Distance (mm)	200; 250; 300; 350
Number of layers	6; 9; 12; 15
Gun speed (mm/s)	100; 150; 200; 250
Powder feed rate (%)*	20; 30; 40; 50
Substrate	Carbon steel 1045; stainless steel 316L
Ratio (O_2 NLPM/H_2 NLPM)**	Oxidant (130 / 570); reductive (147 / 717)

*The powder feed rate is given by the equipment as the feedstock speed rotation in vol. %. The 100 vol. % of the feedstock disc speed rotation is equivalent to 2.15 g/s.

**NLPM, Normalized Liter Per Minute.

Table 2. Spraying conditions according to the Taguchi Experimental Design Method.

Sample	Spraying Distance (mm)	Number of Layers	Gun Speed (mm/s)	Powder feed rate (%)	Substrate	(O_2/H_2) Ratio
1	200	6	100	20	1045	(Red.)
2	200	9	150	30	1045	(Oxi.)
3	200	12	200	40	316L	(Red.)
4	200	15	250	50	316L	(Oxi.)
5	250	6	150	40	316L	(Oxi.)
6	250	9	100	50	316L	(Red.)
7	250	12	250	20	1045	(Oxi.)
8	250	15	200	30	1045	(Red.)
9	300	6	200	50	1045	(Oxi.)
10	300	9	250	40	1045	(Red.)
11	300	12	100	30	316L	(Oxi.)
12	300	15	150	20	316L	(Red.)
13	350	6	250	30	316L	(Red.)
14	350	9	200	20	316L	(Oxi.)
15	350	12	150	50	1045	(Red.)
16	350	15	100	40	1045	(Oxi.)

*(Red.) Reductive ratio, (Oxi.) Oxidant ratio.

2.3. Coating characterization

The quality analysis of the manufactured coatings was performed using microstructural characterization techniques. The cross-sections of the coatings were analysed by Optical Microscopy, OM, Leica DMR (Leica, Germany, Europe) and by Scanning Electron Microscopy, SEM, Hitachi S-3400N (Hitachi High-Technologies, UK, Europe) equipped with an Energy Dispersive X-Ray Spectrometer, EDS, Bruker AXS Xflash Detector 5010 (Bruker, Germany, Europe).

The porosity and thickness of the coatings were calculated by using an image analyser software (Image Pro Plus) on the cross section of the samples at least at five different zones.

Coating adhesion tests were performed using a Posi Test AT-A (Automatic Adhesion Tester) DeFelsko equipment (DeFelsko, NY, USA), according to the ASTM D4541-02 regulation. The hardness measurement was carried out using a Vickers Buehler Micromet 2103 durometer (Buehler, Illinois, USA) with loads of 500 g ($HV_{0.5}$) for 15 s.

2.4. Variance analysis

In order to evaluate the significance of the different spraying parameters on each studied property, a statistical analysis of variance (ANOVA) was used. This measurement allows to identify what parameters interact amongst themselves and to evaluate their significance. To do so, the General Linear Model (GLM) was carried out. The summary of degree of freedom (*DF*), F-ratio (*F*), probability of the null hypotheses (*p*) and percentage of contribution for each factor (*P*) were calculated.

The percentage of contribution (*P*) from each factor was calculated as follows:

$$P\ (\%) = (SS_{factor}/Total\ SS) \times 100 \quad (1)$$

where the SS_{factor} represents the sum of squares for each factor.

The *p* value indicates the probability of the null hypothesis to be rejected as false, i.e., it points if all the spraying variables used are of the same significance. If $p < \alpha$, where $\alpha = 0.05$, the null hypothesis of the no significance of the variable can be rejected. Higher 'F' value suggests that the effect of a factor is larger compared to the error variance suggesting an important parameter influencing the quality characteristics.

3. Results and discussion

3.1. Coating characterization

To optimise the HVOF spraying variables, the Ti coatings produced were analysed to evaluate their principal physical characteristics, microstructure and mechanical properties. Table 3 shows the average values of thickness, porosity, adhesion and microhardness of each coating. These values were obtained from a cross sectional cut of the sample by 10 random measurements of at least 2 coatings obtained under the same conditions. The adhesion values were obtained by taking at least three measurements for each condition. Moreover, the roughness value after sandblasting of each steel was measured. The average roughness value for stainless steel substrates was 5.6 ± 0.3 μm, while a very similar average value, 5.2 ± 0.3 μm, was obtained for carbon steel substrates.

As shown in Table 3, the variation of the spraying parameters in the HVOF process enabled coatings with a broad range of thicknesses, from 138 to 1619 μm, in conditions 10 and 16 respectively. These differences can be observed in the micrographs shown in Figure 2.

The degree of porosity of the different coatings ranges from 2.0 to 13.5 %. As shown in Figures 2 and 3, the porosity is mainly found in the upper area of the coating. This is due to the effect of the deposition of one layer on top of the other, which deformed the previously deposited ones reducing their porosity. For this reason, the last deposited layers present less compaction, and therefore, more porosity. For conditions 3, 11 and 15, the porosity is also observable in the substrate-coating interphase as shown in Figure 3b.

To evaluate the adhesion of the coatings (shown in Table 3) it was necessary to analyse the type of breakage produced: between coating layers (delamination), on the substrate-coating inner face or the bonding, by observing the fractured surface areas. The results showed bonding resistance values of an average of 20 MPa. For conditions 1, 4, 7, 9 and 10, the coating was completely separated from the substrate, indicating the breakage of the bonding. The delamination phenomenon was observed in conditions 8, 11 and 15. This could be due to the fact that in conditions 11 and 15, porosity was located in the lower area of the coating, which caused this type of breakage.

The microhardness of the coatings, gathered in Table 3, indicates an average value of 110 $HV_{0.5}$, with highly dispersed results. Coatings presented zones with different level of porosity. For this reason, the microhardness values vary depending on the zone tested, leading to an average microhardness value with high dispersion.

Table 3. Average microstructural and mechanical values of the coatings.

Sample	Thickness (μm)	Porosity (%)	Adhesion (MPa)	Microhardness ($HV_{0.5}$)
1	487 ± 17	8.0 ± 4.2	19.6 ± 1.7	152 ± 19
2	555 ± 14	13.5 ± 4.8	16.9 ± 1.6	118 ± 13
3	898 ± 92	11.2 ± 4.6	29.0 ± 2.1	156 ± 16
4	512 ± 34	10.2 ± 3.8	14.4 ± 1.5	109 ± 18
5	611 ± 84	7.2 ± 2.5	14.1 ± 1.9	126 ± 18
6	1511 ± 18	3.4 ± 1.8	21.0 ± 0.9	136 ± 10
7	878 ± 24	2.3 ± 2.2	16.2 ± 1.5	113 ± 19
8	718 ± 41	8.1 ± 3.8	18.9 ± 1.2	127 ± 13
9	681 ± 64	4.4 ± 3.4	9.2 ± 1.4	91 ± 21
10	138 ± 75	10.0 ± 3.6	21.6 ± 1.7	140 ± 14
11	1074 ± 39	2.3 ± 1.8	13. 9 ± 0.8	70 ± 26
12	600 ± 53	2.0 ± 2.2	14. 3 ± 1.0	64 ± 17
13	189 ± 29	9.5 ± 3.8	21. 6 ± 1.3	106 ± 15
14	255 ± 31	13.4 ± 5.9	18.8 ± 1.4	127 ± 14
15	1422 ± 13	4.1 ± 0.9	5. 5 ± 0.9	69 ± 24
16	1619 ± 24	3.9 ± 1.3	8.0 ± 1.1	96 ± 24

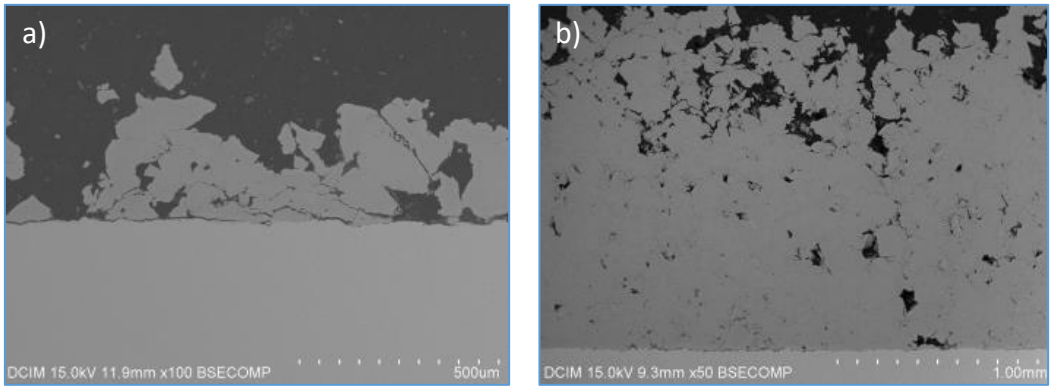

Figure 2. SEM-BSE micrographs of the cross-sectional cuts of the coatings under conditions a) 10 and b) 16.

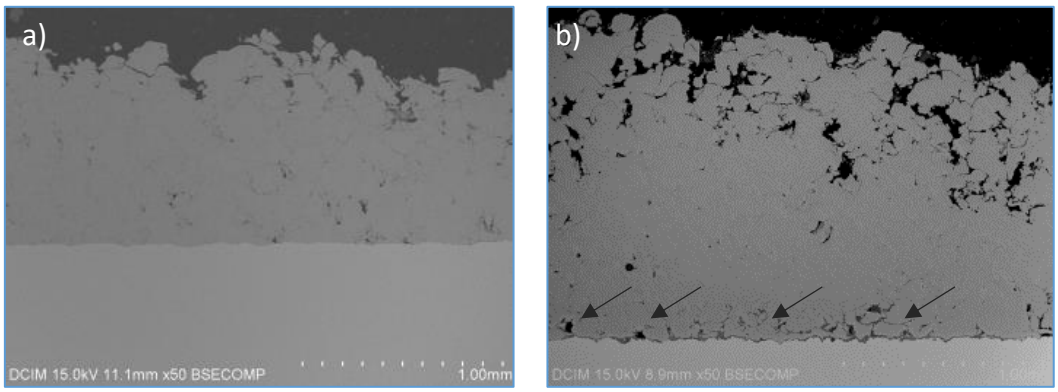

Figure 3. SEM-BSE micrographs of the cross-sectional cuts of the coatings under conditions a) 7 and b) 15.

3.2. Influence of the HVOF process parameters on the thickness of the coatings based on the Taguchi experiment design method.

Figure 4 shows the dependence of the thickness on the HVOF parameters (spraying distance, number of layers, gun speed, powder feed rate, type of substrate and O_2/H_2 ratio employed) using the Taguchi method. The horizontal line indicates the average value. The analysis of the results allowed to obtain the following conclusions referred to the thickness of the titanium coatings deposited: (i) is greater with spraying distances of 250 and 350 mm, (ii) increases with the number of layers, up to a maximum value for 12 layers, (iii) decreases as the gun speed increases, (iv) increases as powder feed rate increases, (v) is slightly greater using carbon steel as a substrate and (vi) is practically independent to the O_2/H_2 ratio used. Therefore, the parameters that most influenced the thickness of the deposited coatings are spraying distance, number of layers, gun speed and powder feed rate.

Spraying distance is a parameter that considerably influences the thickness and quality of the coating and it is affected by the characteristics of the powder supplied. At short distances, the number of particles that rebound and do not get adhered is greater, which implies a thickness reduction. The hammering effect consolidates the coating. However, when the spraying distance increases, two different phenomena take place: firstly, due to the less rebounding of particles, thicker coatings are obtained [25]; secondly, the powder remains longer times in the torch, thus acquiring greater fluidity and, as a result, the deformation of the particles is higher, leading to coatings with a lower thickness and better compaction. The thickness of the produced coating varies according to the predominance of each phenomena depending on the distance, as shown in Figure 4.

As expected, thickness raises when the number of layers increases. The higher the speed of the spraying gun on the substrate, the lower the time that the torch stays on a particular area. Consequently, **the amount of powder sprayed in each zone is inferior and therefore, the deposited coating temperature is also lower**. Accordingly, as observed in Figure 4, higher gun speeds lead to less thick and consistent coatings [26].

When the power feed rate is increased, a greater amount of material is deposited and thicker coatings obtained, as shown in Figure 4. Moreover, by using the carbon steel 1045 as substrate, the obtained thickness is slightly superior compared to the stainless steel 316L. Finally, the O_2/H_2 ratio used have no influence on the thickness, being both conditions close to the horizontal line that represents the average value.

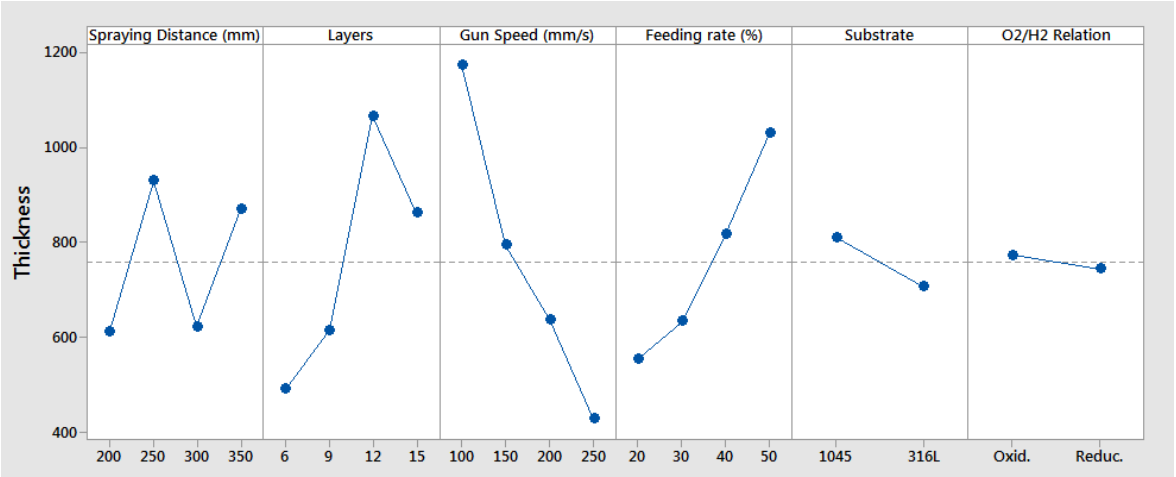

Figure 4. Dependence of coating thickness (μm) on the spraying parameters.

To calculate the percentage of contribution of each spraying parameter and to determine whether all the variables have the same significance, a variance analysis (ANOVA) was performed relating to the thickness of the coating (Table 4). Attending to the results, it can be determined that the type of substrate and the O_2/H_2 ratio are not significant variables for the thickness of the coating, as $p > \alpha$ where $\alpha = 0.05$. It was also observed that the parameter that most contributed to thickness was the gun speed (38.4 %), followed by the number of layers (25.5 %), the powder feed rate (17.3 %) and the spraying distance (10.5 %).

Figure 5a shows the thickness of the coatings in relation to the two most influential parameters: gun speed and number of layers. As observed, the thickest coatings are those obtained with the highest number of layers and at lower gun speeds. In Figure 5b it is also observable that when the spraying distance decreases, two different phenomena take place: firstly, due to the high rebounding of particles, thinner coatings are obtained; secondly, the powder remains less time in the torch, thus particles have less time to absorb heat, reaching the substrate less deformed and coatings are thicker and more porous. Moreover, when the distance increases these two same phenomena appear presenting the opposite effect. The greatest influence of one or another phenomenon varies with the spraying distance as shown in Figure 4. For this reason, in order to obtain coatings with the same thickness, the use of shorter spraying distances and the deposition of an intermediate number of layers would be more appropriate due to the fact that a lower amount of supplied powder leads to a reduction in the final cost of the resulting coatings.

Table 4. Results obtained from ANOVA – Thickness.

Factors	Thickness (μm)				
	DF	Seq. (SS)	F	p	Percentage of contribution
Spraying distance	3	971255	17.00	<0.001	10.5
Number of layers	3	2362180	41.34	<0.001	25.5
Gun Speed	3	3551022	62.14	<0.001	38.4
Powder feed rate	3	1603218	28.06	<0.001	17.3
Substrate	1	131903	6.92	0.013	1.4
$0_2/H_2$ ratio	1	9833	0.52	0.478	0.1
Error	33	628573			6.8
Sum	47	9257983			100.0

DF, Degree of Freedom; Seq. SS, Sequential sum of squares; F, statistical test; p, statistical value.

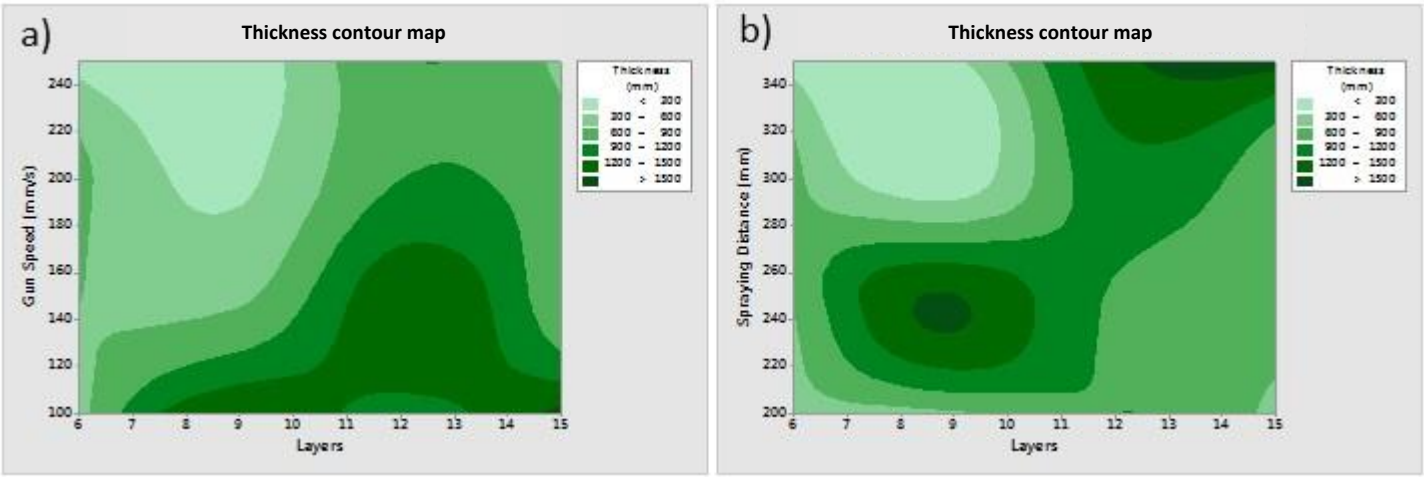

Figure 5. Contour map of coating thickness (µm) in relation to (a) gun speed (mm/s) and number of layers and (b) spraying distance (mm) and number of layers.

3.3. Influence of the HVOF process parameters on the porosity of the coatings using the Taguchi experimental design method.

Figure 6 shows the dependence of the porosity on the HVOF parameters (spraying distance, number of layers, gun speed, powder feed rate, type of substrate and O_2/H_2 ratio employed) using the Taguchi method. The horizontal line indicates the average value. Based on the analysis carried out according to the design of experiments, the following conclusions can be reached with regard to the porosity of the titanium coatings produced: (i) the minimum value was obtained using a spraying distance of 300 mm, (ii) reduces according to the increase in the number of layers, (iii) increases with greater gun speed; (iv) decreases as the powder feed rate increases, (v) decreases when a carbon steel substrate is used and (vi) may be considered independent to the type of gas ratio employed.

In this case, the type of substrate and the gas ratio had practically no effect on the degree of porosity of the produced coatings.

As the spraying distance increases, the particles remain longer time in the flame, producing greater deformation of the powder due to its greater flow resulting from the higher temperature reached. The result would be a coating with a low degree of porosity, up to a certain distance. At 350 mm, the opposite effect takes place. Two possible reasons will be the cooling of the powder particles when moving away from the torch and the slowing of the particles with greater distance [25]–[28].

The deposition of a greater number of layers of material tends to produce denser coatings. It was due to the hammering effect of the layers deposited on top, which reduced the porosity of the layers underneath [27], [29]–[31]. At 9 layers, a maximum of porosity was reached, which can be explained by the lack of uniformity of the conditions 2 and 14. These coatings are not continuous, as observed in Figure 7, complicating the porosity measurement.

Further analysis of the graph reveals that the porosity increases with the gun speed [32]. **This is due to the inferior time that the torch remains in each area and, therefore, the amount of the sprayed powder is lower, providing an inferior deposited coating temperature.** As a result, the particles cool more rapidly and their capacity to deform decreases, giving rise to coatings with

greater porosity. In addition, the torch remains less time in a particular area producing a decrease in the temperature of the substrate.

The use of a higher powder feed rate implies that the number of hot sprayed particles that are able to impact, deform and accumulate to form a layer is greater. Consequently, the obtained coatings are denser. The minimum percentage of porosity reached in this research was found using 50 % of powder. The explanation is based on the ability of the new sprayed powder to compact the previously deposited powder.

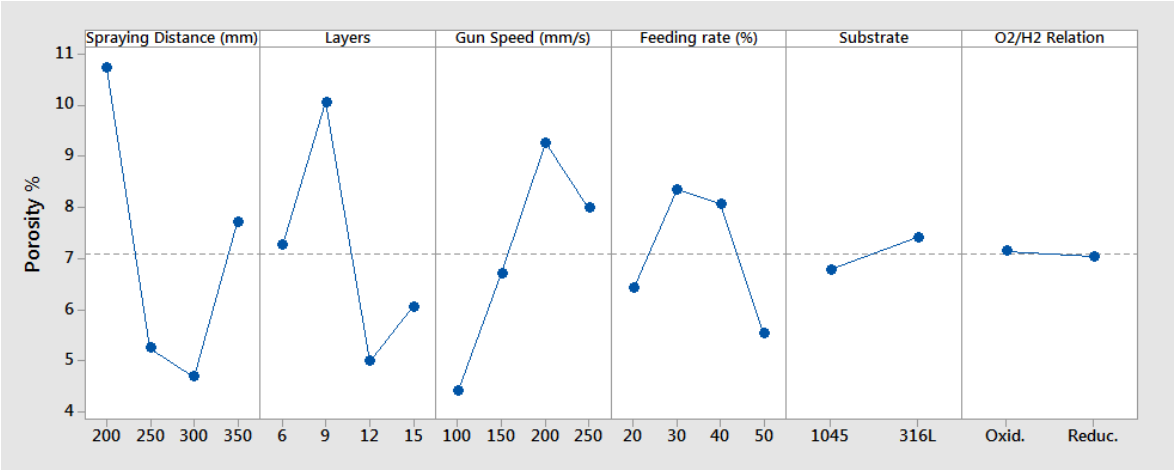

Figure 6. Dependence of coating porosity (%) on the spraying parameters.

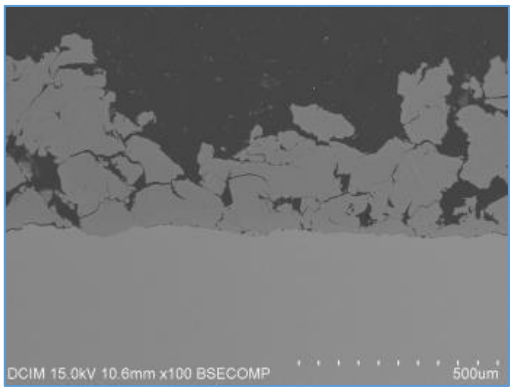

Figure 7. SEM-BSE micrographs of the cross sectional cut of the coating under condition 14.

Table 5 shows, by means of the ANOVA tool, that the significant variables with respect to the porosity of the coatings are the spraying distance and the number of layers. It was also observed that the parameters with the biggest contribution were the spraying distance (25.5 %), followed by the number of layers (15.9 %) and the gun speed (14.2 %). The contribution of error for porosity is the result of the differences in porosity in each zone of the coating: high porosity was observed in the substrate-coating interface due to the high cooling speed of the system which does not favour the plastic deformation of the particles (indicated by arrows in Figure 3b), while in the inner side of the coatings, few pores were observed due to the compacting effect of the layers deposited on top, which reduced the porosity of the layers underneath (Figure 3b).

Figure 8a shows the contour map of the porosity of the coatings related to the two most influential parameters (spraying distance and number of layers) and the ideal conditions with respect to distance and number of layers that should be used according to the porosity is demonstrated. For high degree of porosity, it would be recommended the use of larger or very short spraying distances and the deposition of few layers. In Figure 8b, that shows the degree of porosity in terms of gun speed and number of layers, it can be observed that combining low gun speeds with a high number of layers provides coatings with a small degree of porosity. By comparing Figure 5b and Figure 8a, it is possible to establish that when the coating thickness increases, the porosity decreases.

Table 5. Results obtained from ANOVA – Porosity.

Factors	Porosity (%)				
	DF	Seq. (SS)	F	p	Percentage of contribution
Spraying distance	3	272.75	7.38	<0.001	25.5
Number of layers	3	171.38	4.64	<0.008	15.9
Gun Speed	3	153.35	4.15	0.013	14.2
Powder feed rate	3	64.41	1.74	0.177	6.1
Substrate	1	4.83	0.39	0.535	0.4
$0_2/H_2$ ratio	1	0.13	0.01	0.918	0.01
Error	33	406.64	2.66		37.9
Sum	47	1073.49			100.0

DF, Degree of Freedom; Seq. SS, Sequential sum of squares; F, statistical test; p, statistical value.

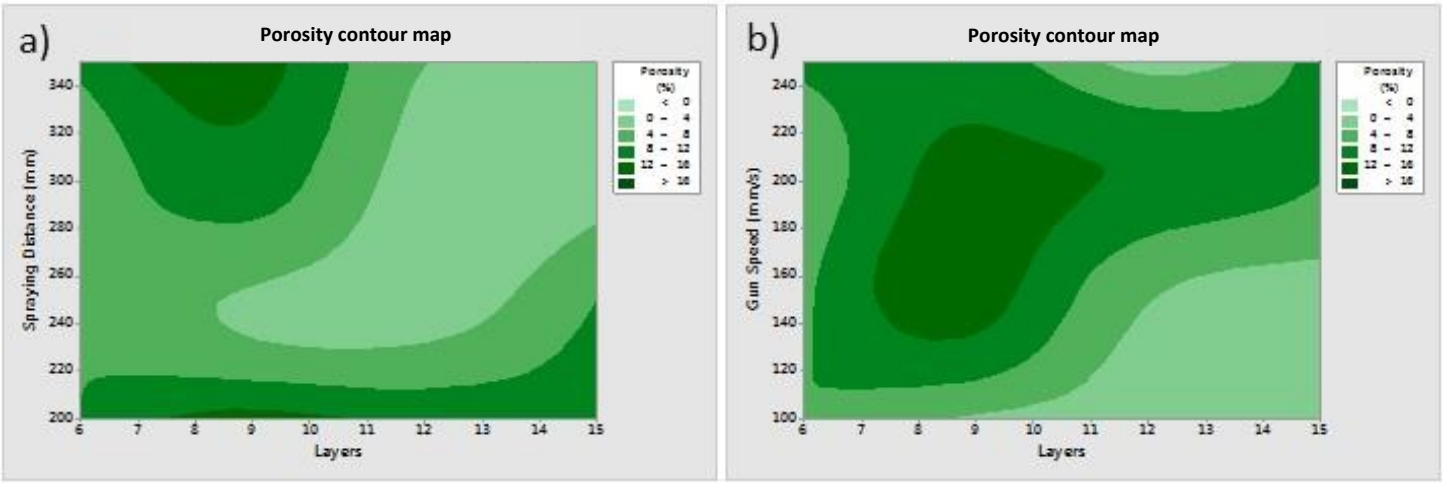

Figure 8. Contour map of coating porosity (%) in relation to (a) spraying distance (mm) and number of layers and (b) gun speed (mm/s) and number of layers.

3.4. Influence of the HVOF process parameters on the coating adhesion using the Taguchi experiment design method.

Figure 9 shows the dependence of the coating adhesion on the HVOF spraying parameters (spraying distance, number of layers, gun speed, powder feed rate, type of substrate and O_2/H_2 ratio used) using the Taguchi method. Again, the horizontal line indicates the average value. It can

be observed that the trends are not well defined in certain parameters. In conditions 3, 13 and 14 the failure is localized between the coating and the adhesive used for testing. For the conditions 1, 4, 7, 9 and 10, the failure took place between the coating and the substrate. Conditions 8, 11 and 15 failed by delamination between the sprayed layers. And finally, in conditions 2, 5, 6, 12 and 16, the substrate-coating adhesion was not homogeneous. In some zones, the fracture took place between the substrate and the coating, while in others, the failure was placed among the first deposited layers.

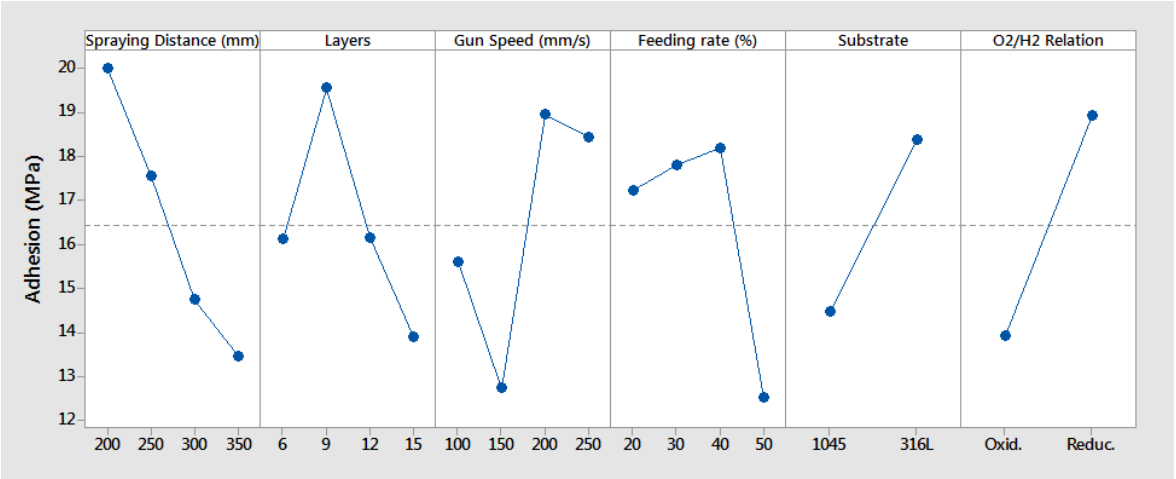

Figure 9. Dependence of the coating adhesion (MPa) on the spraying parameters.

As observed in Figure 9, the substrate-coating adhesion: (i) decreases with an increase in the spraying distance, (ii) decreases with an increase in the number of layers, (iii) has a maximum value for a gun speed of 200 mm/s, (iv) decreases as the powder feed rate increases, (v) is greater employing stainless steel as the substrate, and (vi) increases when the reductive gas ratio (Red.) is used.

At shorter spraying distances, the particles stay shorter times in the flame, their temperature is lower and there are some partially molten particles. Moreover, the particles impact with higher energy. All this produces high bonding strength coatings [33], [34]. The resistance of the bonds of the coatings generated by HVOF largely depends on the state of fusion and size of the particles, more than on their speed or temperature. The complete fusion of the sprayed particles does not contribute to an increase in the bonding of metallic coatings [32]. However, the use of larger, partly molten particles substantially improves the bonding strength, when the particles are in a dual state (liquid-solid). The high speed of the partly molten particles produces plastic deformation on the substrate surface, leading to a high degree of mechanical anchoring between the deposited material and the substrate and thus contributing to a correct bonding [35]. In addition to the mechanical anchoring, the appearance of a physical or chemical bond between the substrate and the coating may take place, producing a greater bonding strength of the coatings produced by HVOF [36]–[38]. The mechanical anchoring mechanism is related to the surface roughness of the substrate and the solidification of the particles impacting [28], [32], [34], [38]–[41].

The number of sprayed layers can modify the building process of each coating, showing different adhesion values [38]. When coating takes place with successive layers, delamination or detachment may occur due to oxidation, internal stress, joining of pores, etc. Therefore, if the spray

of successive layers does not produce more compact coatings, the use of a lower number of layers is recommended.

The higher the gun speed, the lower the heating of the substrate and coating, as well as the amount of the sprayed powder in each area and its temperature, being in a partly molten state. This promotes a greater mechanical impact of the particles on the substrate and the previously deposited layers, favouring the physical bond between the coating and substrate, in addition to the mechanical anchoring mechanism, giving rise to higher adhesion values.

By increasing the powder feed rate, the amount of sprayed material at the same time increases, producing a greater impact and, therefore, favouring the mechanical anchoring. However, the conditions corresponding to 50 % of supplied powder show porosity in the area closest to the substrate, which decreases the adhesion values and brake the trend that implies superior adhesions for greater amounts of powder.

With regard to the type of substrate employed, carbon steel produces lower adhesion values. This is due to the formation of oxide layers in the substrate-coating inner surfaces, which reduces the tensile strength and weakens the adhesion. Figure 10 shows the BSE-SEM image and the EDS mapping of the substrate-coating inner surface on stainless steel. In this case, the presence of oxides between the substrate and the coating is negligible. Figure 11 represents the BSE-SEM image and the EDS mapping of the carbon steel substrate-coating inner surface. Using this substrate, an oxide layer can be observed.

Another variable with significant effect on coating adhesion is the volume of gases used for combustion, where a large quantity of gases (O_2/H_2) provides greater adhesion of the coatings onto the substrates. This occurs when the amount of oxygen is 147 NLPM and hydrogen 717 NLPM (Red.). This volume of gases provides higher kinetic and thermal energy to the particles and heats the substrate more intensely, and therefore, the adhesion is favoured [34]. Figures 13c and 13d show how high energy condition, (low spraying distance and high quantity of gases; high gun speed and short spraying distance), produces coatings with the greatest adhesion.

The adhesion is also influenced by the temperature difference between particle and substrate during impact. The particles temperature has a great effect on the coatings microstructure; the temperature evolution with time determines the material solidification kinetics. During solidification process, prior to the deposition of new particles onto the coating, the particles oxidation could be produced. Moreover, there is a relationship between the O_2/H_2 ratio used and the oxide content of the coating [42]. A greater amount of oxygen enhances the melting and compaction of the particles but causing greater oxidation on the particles and on the coating-substrate interface.

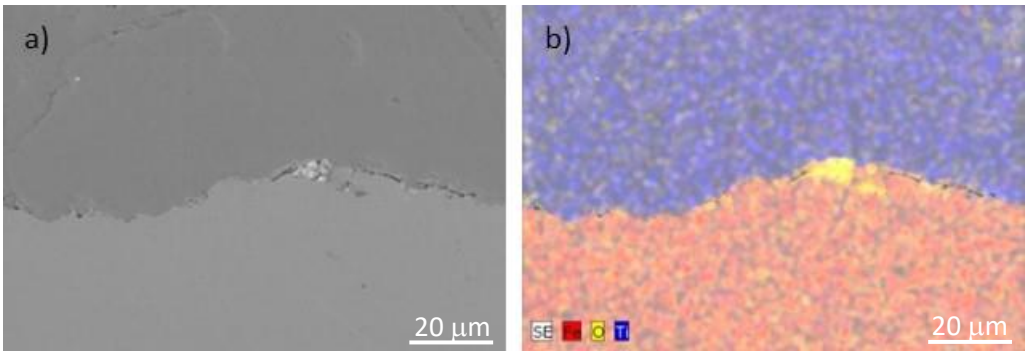

Figure 10. Stainless steel substrate-coating inner surface (condition 12), a) SEM-BSE micrograph, b) EDS mapping.

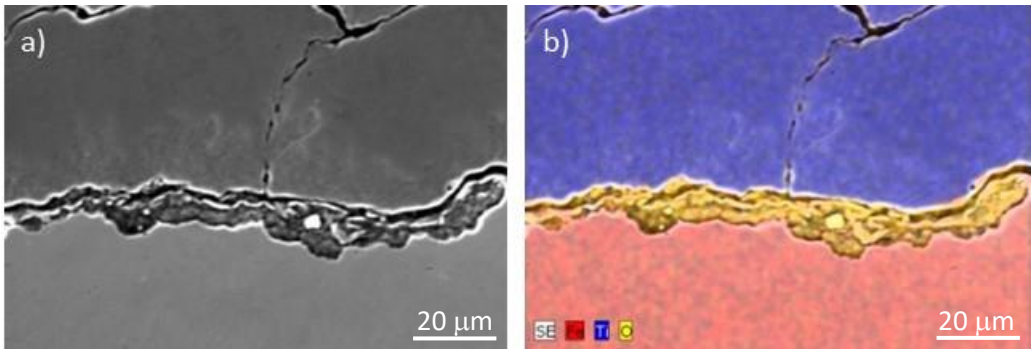

Figure 11. Carbon steel substrate-coating inner surface (condition 15), a) SEM-BSE micrograph, b) EDS mapping.

The ANOVA analysis of the parameters, given in Table 6, shows that all of them have a contribution ranging from 19.9 % to 11.8 %, spraying distance has the highest value.

Figure 12 presents the coating adhesion in function of the significant variables. Firstly, it should be highlighted, as observed in Figures 13a and 13b, that the greatest adhesion is obtained with high gun speeds and elevated powder feed rate, obtained either from the powder feed rate or the number of layers, which supports the above-mentioned theory that greater impact implies greater adhesion.

Table 6. Results obtained from ANOVA- Adhesion.

Factors	Adhesion (MPa)				
	DF	Seq. (SS)	F	p	Percentage of contribution
Spraying distance	3	307.14	196.34	<0.001	19.8
Number of layers	3	196.37	125.52	<0.001	12.6
Gun speed	3	296.96	189.83	<0.001	19.1
Powder feed rate	3	251.98	161.08	<0.001	16.2
Substrate	1	183.69	352.27	<0.001	11.8
$0_2/H_2$ ratio	1	300.30	575.89	<0.001	19.3
Error	33	17.21			1.1
Sum	47	1553.65			100.0

DF, Degree of Freedom; Seq. SS, Sequential sum of squares; F, statistical test; p, statistical value.

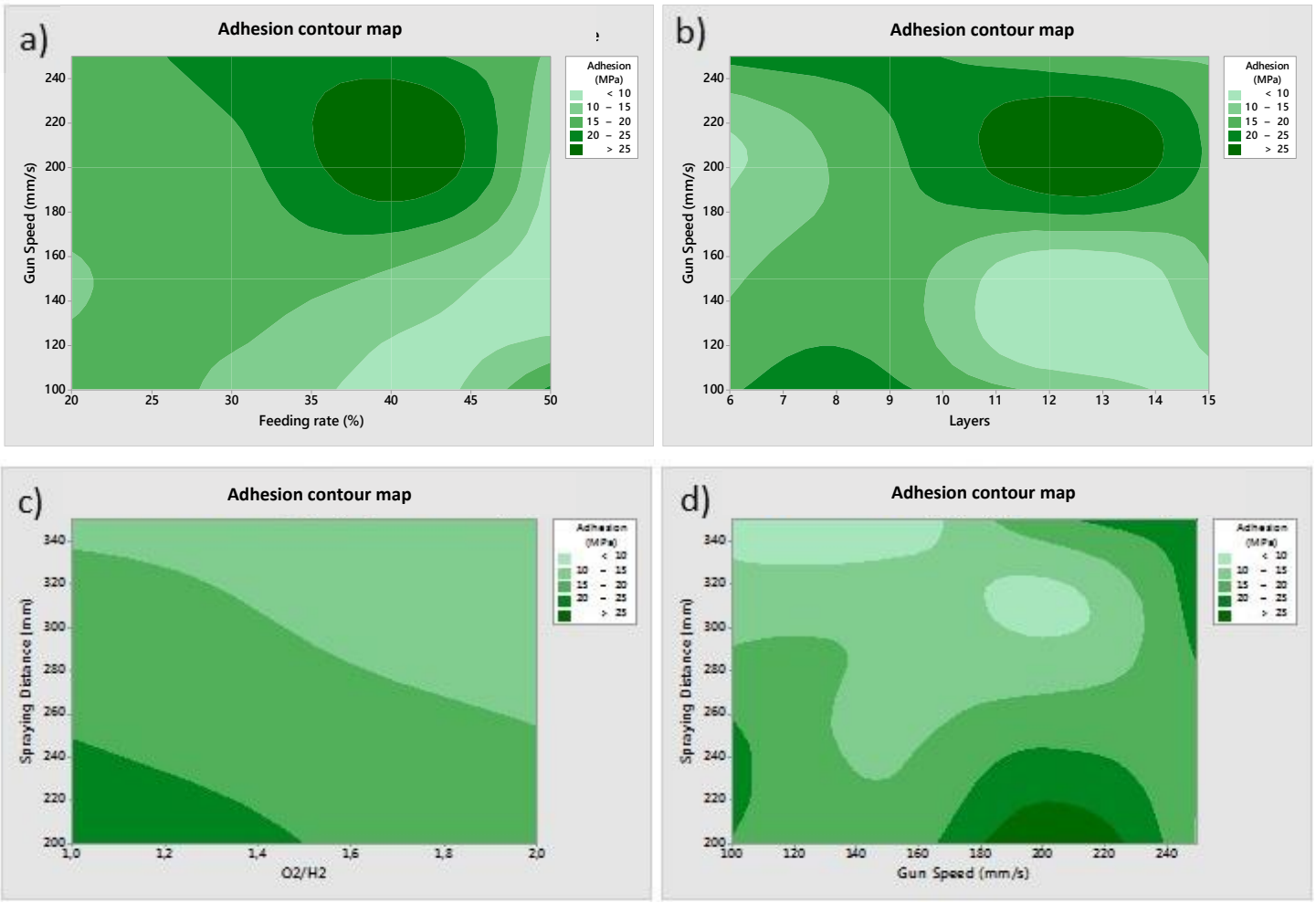

Figure 12. Contour map of coating adhesion (MPa) in relation to (a) gun speed (mm/s) and powder feed rate (%), (b) gun speed (mm/s) and number of layers, (c) spraying distance (mm) and O_2/H_2 ratio and (d) spraying distance (mm) and gun speed (mm/s).

3.5. Influence of the HVOF process parameters on the microhardness of the coatings using the Taguchi experimental design method.

Figure 13 shows the dependence of the microhardness on the HVOF spraying parameters (spraying distance, number of layers, gun speed, powder feed rate, type of substrate and O_2/H_2 ratio used) using the Taguchi method. The horizontal line indicates the average value. As observed in Figure 13, the microhardness of the Ti coatings: (i) decreases as the spraying distance increases, (ii) decreases as the number of layers of material increases, (iii) is greater at higher gun speeds, (iv) has no clear trend with respect to the powder feed rate, (v) may be considered independent to the type of substrate employed, (vi) decreases when the oxidant (Oxi.) ratio is used.

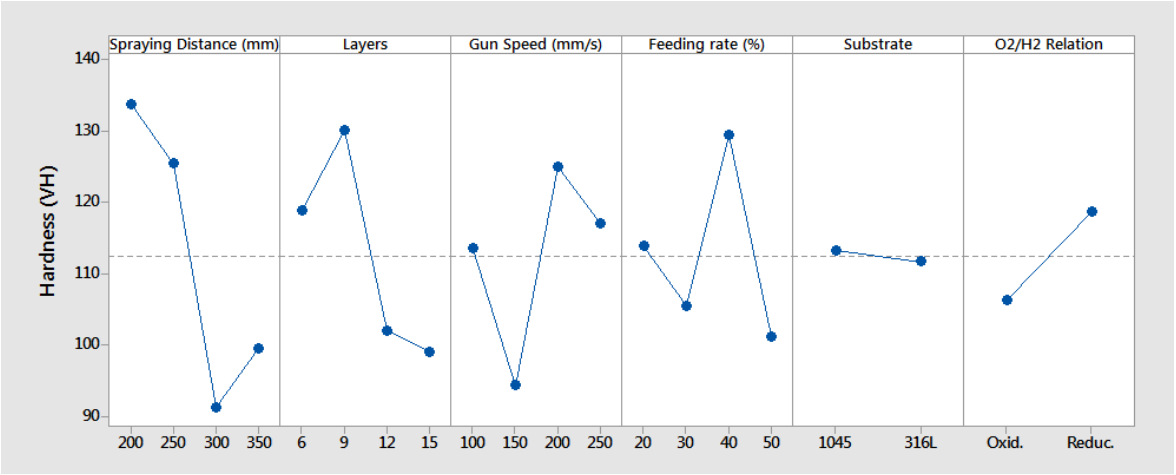

Figure 13. Dependence of the coating microhardness ($HV_{0.5}$) on the spraying parameters.

The inverse relationship between the hardness and porosity of the coatings is a well-known fact [25], [40], [43]–[45]. Accordingly, the coatings deposited using the HVOF technique are expected to obtain a high degree of hardness compared to other spraying techniques, given its capacity to obtain coatings with a low degree of porosity. In this research, the inverse relationship (greater porosity-less hardness) was not always observed and one of the causes could be the heterogeneity of the coatings. The porosity increases as spraying distance increases. The increase in the spraying distance created longer inflight times, which increased the temperature of each individual sprayed powder particle. This higher temperature of the powder favours the oxidation of the particles during the flight because they were immersed in a flame with oxygen at high temperature. The selected load was 0.5 kg to enable the measurement of all coatings and, therefore, to obtain comparable values among the different spraying conditions. Figures 15a and 15b show the residual footprints of two different coatings, with a microhardness of 120 $HV_{0.5}$ and 80 $HV_{0.5}$, respectively. In both cases, the footprint is larger than 50 μm and some of the obtained coatings presented thicknesses of 60 μm.

Another factor that may reduce the coating hardness is the appearance of micro cracks[40]. One of the drawbacks expected of Ti coatings is that they are oxidized and it is well known that these oxides are very fragile. In Figures 14a and 14b cracking was observed after testing, indicating fragility. For this reason, two different mixtures of gases were used, with higher and lower amount of oxygen, to attempt to minimize the quantity of oxide formed. Ti reacts quickly to oxygen to form an oxide layer around the particles. When the oxidised particles collide, the oxide layer hinders the diffusion between them. This fact implies a weaker bond than between two non-oxidised particles of Ti and the hardness of the coating decreases. From the EDS analysis of the sprayed coatings, in Table 7, it is possible to conclude that the differences in the total amount of oxygen between the coatings produced with oxidant and reductive ratio is not remarkable.

When shorter spraying distances are used, the particles reach the substrate at a higher speed. Therefore, they are able to deform and create more compact coatings and, as the powder is in a semi-solid state, hardness is increased by deformation [44]. A linear dependence between the particles speed and the hardness of the resulting coating has been also described [40].

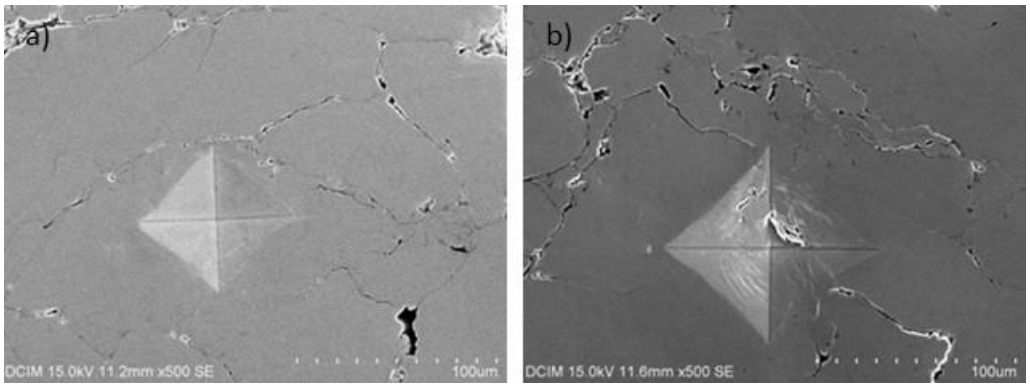

Figure 14. SEM-SE micrographs of indentation footprints (a) condition 7 and (b) condition 9.

Table 7. EDS elemental composition of Ti coatings using the Oxidant and the Reductive ratio.

Sample	Element [wt. %]		Element [at. %]	
	O	**Ti**	**O**	**Ti**
11 (Oxi.)	0.52	99.48	1.55	98.45
12 (Red.)	0.98	99.02	2.87	97.13
15 (Red.)	0.54	99.46	1.59	98.41
16 (Oxi.)	0.66	99.34	1.95	98.05

Table 8 shows the significance of the variables established by ANOVA. For the microhardness, these variables are the spraying distance, number of layers, gun speed, powder feed rate and O_2/H_2 ratio. Nevertheless, the parameters that most contributed were the spraying distance (31.7 %) followed by the number of deposited layers (16.5 %).

As shown in Figure 15, the use of dynamic conditions leads to a compaction and work hardening of the coatings, resulting in higher hardness values. Short spraying distances and high gun speeds (Figure 15a) or elevated powder feed rate (Figure 15b) may be the selected parameters to obtain a coating with the highest value of microhardness.

Table 8. Results obtained from ANOVA - Vickers Microhardness.

Factors	Vickers Microhardness (0.5)				
	DF	Seq. (SS)	F	p	Percentage of contribution
Spraying distance	3	14829.9	15.19	<0.001	31.7
Number of layers	3	7725.0	7.91	<0.001	16.5
Gun Speed	3	6109.2	6.26	0.002	13.0
Powder feed rate	3	5605.2	5.74	0.003	11.9
Substrate	1	29.8	0.09	0.764	0.1
$0_2/H_2$ relation	1	1849.3	5.68	0.023	3.9
Error	33	10736.2	0.90	0.349	22.9
Sum	47	46884.6			100.0

DF, Degree of Freedom; Seq. SS, Sequential sum of squares; F, statistical test; p, statistical value.

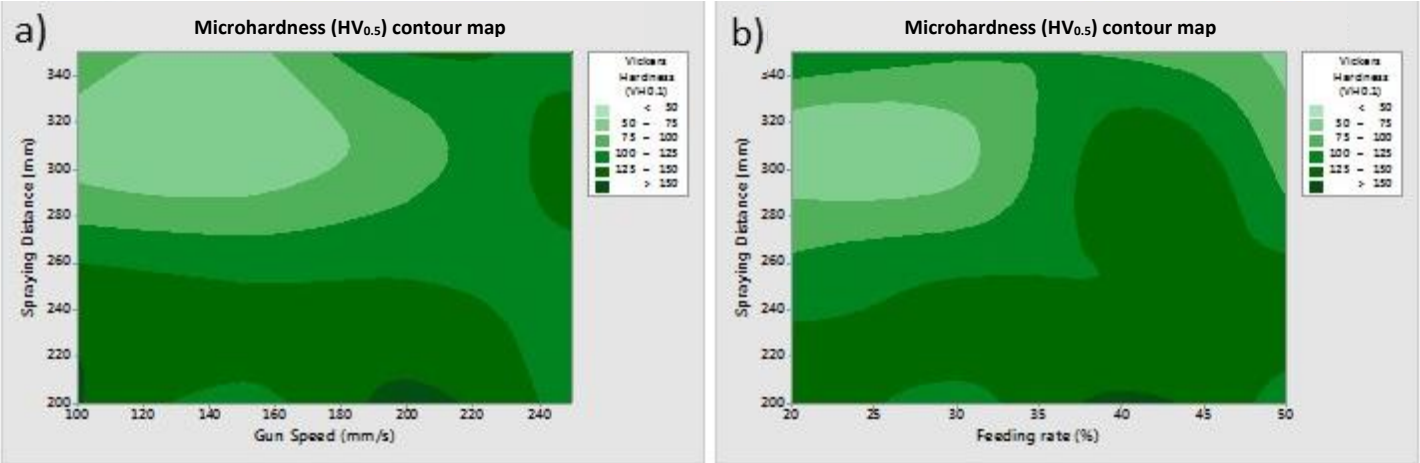

Figure 15. Contour map of the coating microhardness ($HV_{0.5}$) related to the (a) spraying distance (mm) and gun speed (mm/s) and the (b) spraying distance (mm) and powder feed rate (%).

3.6. Summary.

After studying the influence of the spraying variables on the thickness, porosity, adhesion and hardness of the coatings produced, it can be generally concluded that not all the spraying variables affect the different measured properties in the same way. If another property or feature were measured, a different contribution of the spraying parameters could be obtained. However, in all cases, one of the most influential variable was the spraying distance, followed by the number of deposited layers. It is also necessary to differentiate between mechanical properties and characteristics of the coatings, as well as their service requirements, according to their real application.

The contour maps in which the independent value, i.e., the axes used, were layers and gun speed (Figures 5a, 8b and 12 b) reveal that it is possible to achieve simultaneously hard and well adhered coatings that show medium to high porosity and medium thickness by applying about 14 layers and a gun speed of 220 mm/s. These coatings would be adequate for biological applications where the key point is to have a porosity that is compatible with cell growth while being sure of having a system that is not prone to failure by delamination.

Other interesting condition is to have low porosity coatings, which can be achieved by applying about 9 layers, slow gun speed (100 mm/s) and intermediate spraying distances. This ensures also having high adhesion of the coating to the substrate which can be further increased (Figures 8b and 12 b). These conditions would be adequate for coatings in contact to aggressive environments.

The Taguchi approach has been proved as a useful tool to obtain the most appropriate range of conditions based on the property sought for each application.

4. Conclusions

The main conclusions extracted from this research are as following:

1. The Taguchi experiment design is a valid method for an initial approach to establish the variables with greater influence on the characteristics of the Ti coatings deposited by HVOF on the steel substrates. By using this method, the number of required experiments was reduced from 1024 to 16.
2. The analysis of the graphs and contour maps derived from the DOE methodology allows the design of the coatings depending on the desired or required properties in function of the variables of the HVOF spraying technique used.
3. The spraying parameters with the greatest influence on the features and properties of the coatings (from high to low) are: spraying distance, number of layers, gun speed, powder feed rate, type of (steel) substrate and O_2/H_2 ratio.
4. Depending on the spraying conditions, it is possible to produce coatings without cracking and a wide range of thicknesses, low porosity, good continuity between coatings and substrates and different microhardness.
5. The contour map reveals that it is possible to achieve simultaneously hard and well adhered coatings that show medium to high porosity and intermediate thickness by applying high number of layers and gun speed. These coatings would be adequate for biological applications.
6. Other interesting condition would be the obtaining of low porosity coatings, which could be achieved by applying an intermediate number of layers and spraying distance and slow gun speed. This also ensures a high adhesion of the coating to the substrate which can be further increased. These coatings would be adequate for aggressive environments, such as molten aluminium.

ACKNOWLEDGEMENTS

The authors wish to express their gratitude to the Ministerio de Educación, Cultura y Deporte of Spain (15/03606 FPU grant), the Agencia Estatal de Investigación (Project RTI2018-096391-B-C31) and the Comunidad de Madrid (Project ADITIMAT-CM S2018/NMT-4411).

REFERENCES

[1] D. Heim, F. Holler, and C. Mitterer, Hard coatings produced by PACVD applied to aluminium die casting, Surface and Coatings Technology, vol. 116–119, pp. 530–536, 1999. https://doi.org/10.1016/S0257-8972(99)00104-8

[2] C. Mitterer, F. Holler, F.Üstel and D. Heim, Application of hard coatings in aluminium die casting — soldering , erosion and thermal fatigue behaviour, Surface and Coatings Technology, vol. 125, pp. 233–239, 2000. https://doi.org/10.1016/S0257-8972(99)00557-5

[3] K. S. Klimek, A. Gebauer-Teichmann, P. Kaestner, and K. Rie, Duplex-PACVD coating of surfaces for die casting tools, Surface and Coatings Technology, vol. 201, pp. 5628–5632, 2007. https://doi.org/10.1016/j.surfcoat.2006.07.163

[4] S. H. Lee, K. H. Nam, S. C. Hong, and J. J. Lee, Low temperature deposition of TiB2 by inductively coupled plasma assisted CVD, Surface and Coatings Technology, vol. 201, pp. 5211–5215, 2007. https://doi.org/10.1016/j.surfcoat.2006.07.209

[5] R. K. Roy, Design Of Experiments Using Taguchi Approach: 16 Steps to Product and Process Improvement. Wiley. ISBN 0-471-36101-1. https://doi.org/10.1520/JTE12406J

[6] S. K. Madhavi, D. Sreeramulu, and M. Venkatesh, Evaluation of Optimum Turning Process of Process Parameters Using DOE and PCA Taguchi Method, Materials today: proceedings, vol. 4, pp. 1937–1946, 2017. https://doi.org/10.1016/j.matpr.2017.02.039

[7] M. Oksa, E. Turunen, T. Suhonen, T. Varis, and S. Hannula, Optimization and Characterization of High Velocity Oxy-fuel Sprayed Coatings: Techniques, Materials, and Applications, Coatings, vol.1, pp. 17–52, 2011. https://doi.org/10.3390/coatings1010017

[8] S. Fayyazi, M. Kasraei, and M. E. Bahrololoom, Improving Impact Resistance of High-Velocity Oxygen Fuel-Sprayed WC-17Co Coating Using Taguchi Experimental Design, Journal of Thermal Spray Technology, vol. 28, no. 4, pp. 706–716, 2019. https://doi.org/10.1007/s11666-019-00844-6

[9] S. Fayyazi, M. E. Bahrololoom, and M. Kasraei, Optimizing High-Velocity Oxygen Fuel-Sprayed WC–17Co Coating Using Taguchi Experimental Design to Improve Tribological Properties, Transactions of the Indian Institute of Metals, vol. 71, no. 12, pp. 3045–3062, 2018. https://doi.org/10.1007/s12666-018-1406-9

[10] S. Thermsuk and P. Surin, Optimization parameters of WC-12Co HVOF sprayed coatings on SUS 400 stainless steel, Procedia Manufacturing, vol. 30, pp. 506–513, 2019. https://doi.org/10.1016/j.promfg.2019.02.071

[11] A. J. Becker, J. H. Blanks, TiB2-coated cathodes for aluminum smelting cells, Thin Solid Films, vol. 119, pp. 241–246, 1984. https://doi.org/10.1016/0040-6090(84)90009-9

[12] Y. Wang, Application of ceramic thermal spray coatings for molten metal handling tools and moulds. Surface Engineering, vol. 15, pp. 205-209, 1999. https://doi.org/10.1179/026708499101516524

[13] M. Yu, R. Shivpuri, and R. A. Rapp, Effects of Molten Aluminum on H13 Dies and Coatings, Journal of Materials Engineering and Performance, vol. 4, pp. 175–181, 1995. https://doi.org/10.1007/BF02664111

[14] M. U. Pellizzari, A. Molinari, and G. Straffelini, Thermal fatigue resistance of plasma duplex-treated tool steel, Surface and Coatings Technology, vol.142-144, pp.1109-1115, 2001.

https://doi.org/10.1016/S0257-8972(01)01223-3

[15] S. V Shah and N. B. Dahotre, Laser surface-engineered vanadium carbide coating for extended die life, Journal of Materials Processing Technology, vol. 124, pp. 105–112, 2002. https://doi.org/10.1016/S0924-0136(02)00109-7

[16] A. Srivastava, V. Joshi, R. Shivpuri, R. Bhattacharya, and S. Dixit, A multilayer coating architecture to reduce heat checking of die surfaces, Surface and Coatings Technology, vol. 164, pp. 631–636, 2003. https://doi.org/10.1016/S0257-8972(02)00690-4

[17] Y. Wang, A study of PVD coatings and die materials for extended die-casting die life, Surface and Coatings Technology, vol. 94-95, 1997. https://doi.org/10.1016/S0257-8972(97)00476-3

[18] Y. Chu, K. Venkatesan, J. R. Conrad, K. Sridharan, M. Shamim, and R. P. Fetherston, An evaluation of metallic coatings for erosive wear resistance in die casting applications, Wear, vol. 192, pp. 49–55, 1996. https://doi.org/10.1016/0043-1648(95)06749-3

[19] M. Li *et al.*, Porous titanium scaffold surfaces modified with silver loaded gelatin microspheres and their antibacterial behavior, Surface and Coatings Technology, vol. 286, pp. 140–147, 2016. https://doi.org/10.1016/j.surfcoat.2015.12.006

[20] B. Dabrowski, W. Swieszkowski, D. Godlinski, and K. J. Kurzydlowski, Highly porous titanium scaffolds for orthopaedic applications, Journal of Biomedical Materials Research Part B Applied Biomaterials, vol.51, pp. 53-61, 2010. https://doi.org/10.1002/jbm.b.31682

[21] Y. Kirmanidou, M.Sidira, M. Drosou, V. Bennani, A. Bakopoulou, A. Tsouknidas, N. Michailidis, K. Michalakis, New Ti-Alloys and Surface Modifications to Improve the Mechanical Properties and the Biological Response to Orthopedic and Dental Implants : A Review, BioMed Research International, vol.2, pp. 1-21, 2016.

[22] K. Kim, S. Kuroda, M. Watanabe, R. Huang, H. Fukanuma, and H. Katanoda, Comparison of Oxidation and Microstructure of Warm-Sprayed and Cold-Sprayed Titanium Coatings, Journal of Thermal Spray Technology, vol. 21, pp. 550–560, 2012. https://doi.org/10.1007/s11666-011-9703-4

[23] K. Kim, M. Watanabe, J. Kawakita, and S. Kuroda, Effects of Temperature of In-flight Particles on Bonding and Microstructure in Warm-Sprayed Titanium Deposits, Journal of Thermal Spray Technology, vol. 18, pp. 392–400, 2009. https://doi.org/10.1007/s11666-009-9303-8

[24] M. N. Khan and T. Shamim, Investigation of a dual-stage high velocity oxygen fuel thermal spray system, Applied Energy, vol. 130, pp. 853–862, 2014. https://doi.org/10.1016/j.apenergy.2014.03.075

[25] S. H. Zahiri, C. I. Antonio, and M. Jahedi, Elimination of porosity in directly fabricated titanium via cold gas dynamic spraying, Journal of Materials Processing Technology, vol. 209, pp. 922–929, 2008. https://doi.org/10.1016/j.jmatprotec.2008.03.005

[26] L. Gil and M. H. Staia, Influence of HVOF parameters on the corrosion resistance of NiWCrBSi coatings, Thin Solid Films, vol. 421, pp. 446–454, 2002. https://doi.org/10.1016/S0040-6090(02)00815-5

[27] M. Campo, M. Carboneras, M.D. López, B. Torres, P. Rodrigo, E. Otero, J. Rams, Corrosion resistance of thermally sprayed Al and Al / SiC coatings on Mg. Surface and Coating Technology, vol. 203, pp. 3224–3230, 2009. https://doi.org/10.1016/j.surfcoat.2009.03.057

[28] D. Shi, M. Li, and P. D. Christofides, Diamond Jet Hybrid HVOF Thermal Spray : Rule-Based Modeling of Coating Microstructure, Industrial and Engineering Chemistry Research, pp. 3653–3665, 2004. https://doi.org/10.1021/ie030560h

[29] M. Carboneras, M.D. López, P. Rodrigo, M. Campo, B. Torres, E. Otero, J. Rams, Corrosion behaviour of thermally sprayed Al and Al/SiCp composite coatings on ZE41 magnesium alloy in chloride medium, Corrosion Science, vol. 52, 761–768, 2010. https://doi.org/10.1016/j.corsci.2009.10.040

[30] P. Rodrigo, M. Campo, B. Torres, M. D. Escalera, E. Otero, and J. Rams, Microstructure and wear resistance of Al – SiC composites coatings on ZE41 magnesium alloy, Applied Surface Science. vol. 255, pp. 9174–9181, 2009. https://doi.org/10.1016/j.apsusc.2009.06.122

[31] S. García-Rodríguez, B. Torres, A. J. López, E. Otero and J. Rams, Characterization and mechanical properties of stainless steel coatings deposited by HVOF on ZE41 magnesium alloy, Surface and Coatings Technology, vol. 359, pp. 73-84, 2018. https://doi.org/10.1016/j.surfcoat.2018.12.056

[32] Y. Wang, C. Li, and A. Ohmori, Influence of substrate roughness on the bonding mechanisms of high velocity oxy-fuel sprayed coatings, Surface and Coatings Technology, vol. 485, pp. 141–147, 2005. https://doi.org/10.1016/j.tsf.2005.03.024

[33] C. Lyphout, P. Nylén, L. G. Östergren, Relationships Between Process Parameters, Microstructure and Adhesion Strength of HVOF Sprayed IN718 Coatings, Journal of Thermal Spray Technology, vol. 20, pp. 76–82, 2011. https://doi.org/10.1007/s11666-010-9543-7

[34] C. Lyphout, Adhesion Strength of HVOF Sprayed IN718 Coatings, Journal of Thermal Spray Technology, vol. 21, 2012. https://doi.org/10.1007/s11666-011-9689-y

[35] C. Li and G. Yang, Int . Relationships between feedstock structure, particle parameter, coating deposition, microstructure and properties for thermally sprayed conventional and nanostructured WC – Co, International Journal of Refractory Metals and Hard Materials, vol. 39, pp. 2–17, 2013. https://doi.org/10.1016/j.ijrmhm.2012.03.014

[36] C. Li and Y. Wang, Effect of Particle State on the Adhesive Strength of HVOF Sprayed Metallic Coating, Journal of Thermal Spray Technology, vol. 11, pp. 523–529, 2002. https://doi.org/ 10.1361/105996302770348655

[37] Y. Wang, C. Li, and A. Ohmori, Examination of factors influencing the bond strength of high velocity oxy-fuel sprayed coatings, Surface and Coatings Technology, vol. 200, pp. 2923–2928, 2006. https://doi.org/10.1016/j.surfcoat.2004.11.040

[38] C. R. C. Lima and J. M. Guilemany, Adhesion improvements of Thermal Barrier Coatings with HVOF thermally sprayed bond coats, Surface and Coatings Technology, vol. 201, pp. 4694–4701, 2007. https://doi.org/10.1016/j.surfcoat.2006.10.005

[39] D. Sen, N. M. Chavan, D. S. Rao, and G. Sundararajan, Influence of Grit Blasting on the Roughness and the Bond Strength of Detonation Sprayed Coating, Journal of Thermal Spray Technology, vol. 19, pp. 805–815, 2010. https://doi.org/10.1007/s11666-010-9476-1

[40] K. Murugan, A. Ragupathy, V. Balasubramanian, and K. Sridhar, Optimizing HVOF spray process parameters to attain minimum porosity and maximum hardness in WC – 10Co – 4Cr coatings, Surface and Coatings Technology, vol. 247, pp. 90–102, 2014. https://doi.org/10.1016/j.surfcoat.2014.03.022

[41] M. Watanabe, S. Kuroda, K. Yokoyama, T. Inoue, and Y. Gotoh, Modified tensile adhesion test for evaluation of interfacial toughness of HVOF sprayed coatings, Surface and Coatings

Technology, vol. 202, pp. 1746–1752, 2008. https://doi.org/10.1016/j.surfcoat.2007.07.028

[42] N. Abu-warda, A. J. López, M. D. López, and M. V Utrilla, Ni20Cr coating on T24 steel pipes by HVOF thermal spray for high temperature protection, Surface and Coatings Technology, p. 125-133, 2019. https://doi.org/10.1016/j.surfcoat.2019.125133

[43] B. Torres, M. Campo, and J. Rams, Properties and microstructure of Al – 11Si / SiCp composite coatings fabricated by thermal spray, Surface and Coatings Technology, vol. 203, no. 14, pp. 1947–1955, 2009. https://doi.org/10.1016/j.surfcoat.2009.01.021

[44] K. Dobler, H. Kreye, and R. Schwetzke, Oxidation of Stainless Steel in the High Velocity Oxy-Fuel Process, Journal of Thermal Spray Technology, vol. 9, pp. 407–413, 2000. https://doi.org/10.1361/105996300770349872

[45] S. Vignesh, K. Shanmugam, V. Balasubramanian, and K. Sridhar, Identifying the optimal HVOF spray parameters to attain minimum porosity and maximum hardness in iron based amorphous metallic coatings, Defence Technology, vol. 13, no. 2, pp. 101–110, 2017. https://doi.org/10.1016/j.dt.2017.03.001